Perlecan regulates bidirectional Wnt signaling at the *Drosophila* neuromuscular junction

Keisuke Kamimura,[1] Kohei Ueno,[2] Jun Nakagawa,[1] Rie Hamada,[1] Minoru Saitoe,[2] and Nobuaki Maeda[1]

[1]Department of Brain Development and Neural Regeneration and [2]Department of Sensory and Motor Systems, Tokyo Metropolitan Institute of Medical Science, Setagaya-ku, Tokyo 156-8506, Japan

Heparan sulfate proteoglycans (HSPGs) play pivotal roles in the regulation of Wnt signaling activity in several tissues. At the *Drosophila melanogaster* neuromuscular junction (NMJ), Wnt/Wingless (Wg) regulates the formation of both pre- and postsynaptic structures; however, the mechanism balancing such bidirectional signaling remains elusive. In this paper, we demonstrate that mutations in the gene of a secreted HSPG, *perlecan/trol*, resulted in diverse postsynaptic defects and overproduction of synaptic boutons at NMJ. The postsynaptic defects, such as reduction in subsynaptic reticulum (SSR), were rescued by the postsynaptic activation of the Frizzled nuclear import Wg pathway. In contrast, overproduction of synaptic boutons was suppressed by the presynaptic down-regulation of the canonical Wg pathway. We also show that Trol was localized in the SSR and promoted postsynaptic accumulation of extracellular Wg proteins. These results suggest that Trol bidirectionally regulates both pre- and postsynaptic activities of Wg by precisely distributing Wg at the NMJ.

Introduction

Highly coordinated structuring of the pre- and postsynaptic apparatus is essential for synaptic development and plasticity. Trans-synaptic communications mediated by secreted and membrane-bound proteins, such as agrin, Wnt, and neuroligin, play pivotal roles in such coordination (Packard et al., 2003; Dean and Dresbach, 2006; Singhal and Martin, 2011). Among these, Wnt signalings have been implicated in the formation and plasticity of synaptic connections in the central nervous system (CNS) and neuromuscular junction (NMJ) of both vertebrates and invertebrates (Salinas and Zou, 2008; Budnik and Salinas, 2011). Recent genetic studies on *Drosophila melanogaster* began to elucidate the molecular mechanism of Wnt signaling in developing larval NMJs, a widely used model of glutamatergic synapse that shows many similarities to the excitatory synapses in mammalian CNS. At *Drosophila* NMJ, Wnt/Wingless (Wg) is secreted from the motor axon terminals and binds to the receptor *Drosophila* Frizzled-2 (DFz2), which is localized on both pre- and postsynaptic membranes (Packard et al., 2002). Wg presynaptically activates the local canonical pathway involving Dishevelled (Dsh) and Shaggy (Sgg), a *Drosophila* homologue of glycogen synthase kinase 3β, and promotes the proliferation of synaptic boutons (Miech et al., 2008). On the other hand, in the postsynaptic muscle fibers, Wg activates the Frizzled nuclear import (FNI) pathway, in which Wg induces the cleavage of the C terminus of DFz2 (DFz2-C). The DFz2-C is then transported into muscle nuclei and promotes postsynaptic differentiation (Mathew et al., 2005; Mosca and Schwarz, 2010). Thus, Wg signaling has bidirectional activity coordinating the development of pre- and postsynaptic apparatus during rapid growth of larval muscle fibers.

Complicated machinery is required to achieve such bidirectional signaling because Wg is highly hydrophobic owing to palmitoyl modifications. Recently, it was revealed that Wg is released from the presynaptic terminals by exosome-like vesicles containing the Wnt-binding protein Evenness interrupted (Evi; Korkut et al., 2009). Evi plays critical roles both in the presynaptic secretion of Wg via exosomes and in the postsynaptic trafficking of DFz2 to the muscle nuclei. However, little is known about the mechanism by which Wg proteins are properly

Correspondence to Nobuaki Maeda: maeda-nb@igakuken.or.jp

Abbreviations used in this paper: BMP, bone morphogenetic protein; BRP, Bruchpilot; CNS, central nervous system; DFz2, *Drosophila* Frizzled-2; DLG, Discs large; Dlp, Dally-like glypican; Dsh, Dishevelled; dsRNA, double-stranded hairpin RNA; eEJP, evoked excitatory junction potential; Evi, Evenness interrupted; FNI, Frizzled nuclear import; Gbb, Glass bottom boat; HS, heparan sulfate; HSPG, HS proteoglycan; KO, knockout; mEJP, miniature excitatory junction potential; NMJ, neuromuscular junction; *sfl*, *sulfateless*; Sgg, Shaggy; SSR, subsynaptic reticulum; Trol, terribly reduced optic lobes; UAS, upstream activation sequence; Wg, Wingless.

The Rockefeller University Press $30.00
J. Cell Biol. Vol. 200 No. 2 219–233
www.jcb.org/cgi/doi/10.1083/jcb.201207036

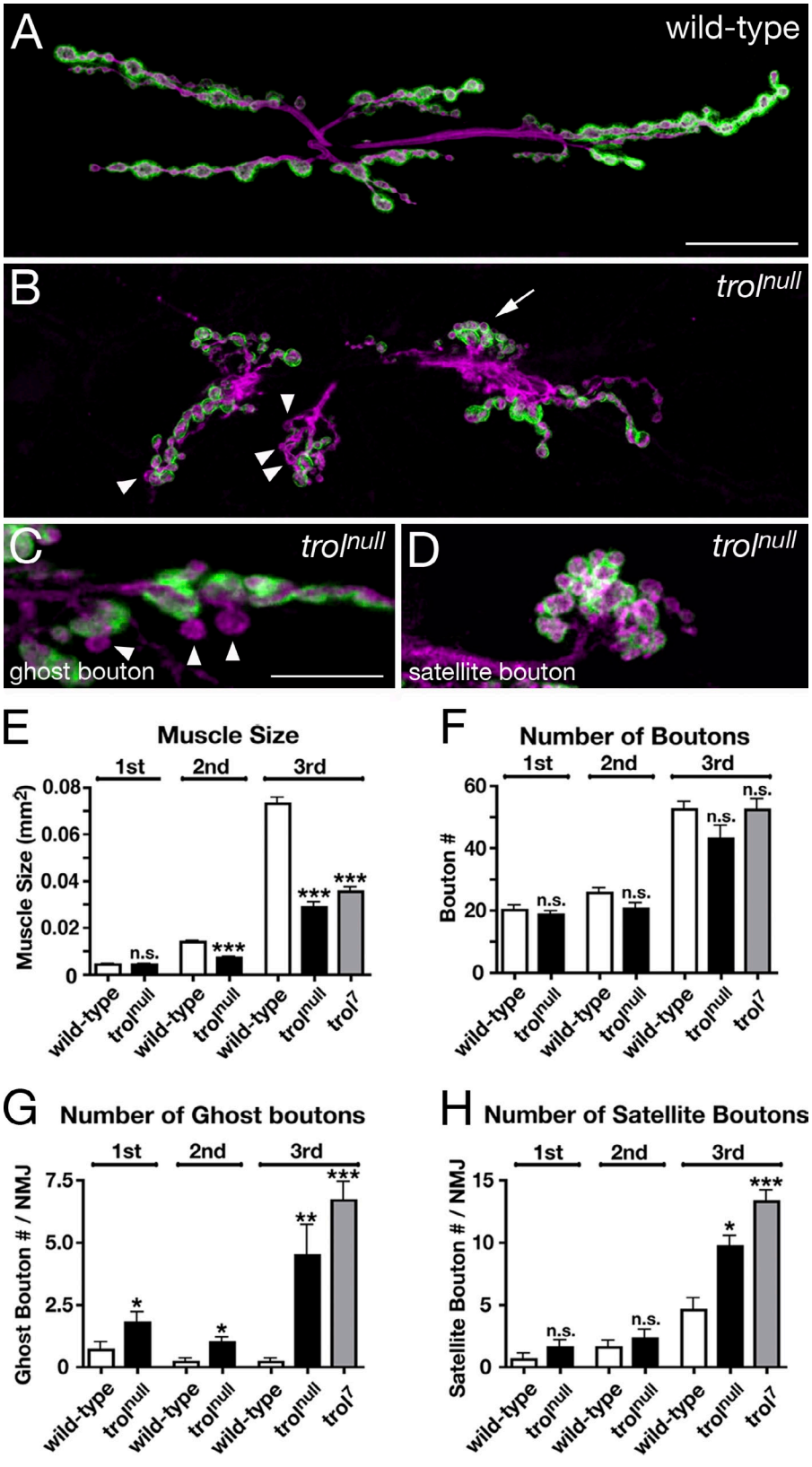

Figure 1. ***trol* mutations affect both muscle size and NMJ morphology.** (A–D) Type I boutons of wild-type (A) and *trol*^{null} mutant (B–D) larvae were stained with anti-HRP (magenta) and anti-DLG (green) antibodies. *trol* mutants showed ghost (arrowheads in B and C) and satellite boutons (B, arrow; and D). (E–H) Area of muscle 6/7 (E), total number of boutons (F), and numbers of ghost (G) and satellite (H) boutons in the NMJs of the first-, second-, and third-instar larvae of wild-type and *trol* (*trol*^{null} and *trol*^{7}) mutants were measured. Error bars represent SEM (n = 10; *, $P < 0.05$; **, $P < 0.01$; and ***, $P < 0.001$ relative to wild type). Bars: (A) 30 µm; (C) 12 µm.

transported across the synaptic clefts and allocated to both pre- and postsynaptic membranes at the NMJ.

Previous studies showed that Wnt/Wg proteins bind to heparan sulfate (HS) proteoglycans (HSPGs) via HS chains, the interactions of which play critical roles in Wnt/Wg signaling. In particular, cell surface HSPGs are required to form the stable long-range gradient of Wnt/Wg, which specifies distinct cell fates in a concentration-dependent manner during morphogenesis of various organs (Lin, 2004; Gallet et al., 2008; Kikuchi et al., 2011). Thus, we hypothesized that HSPGs

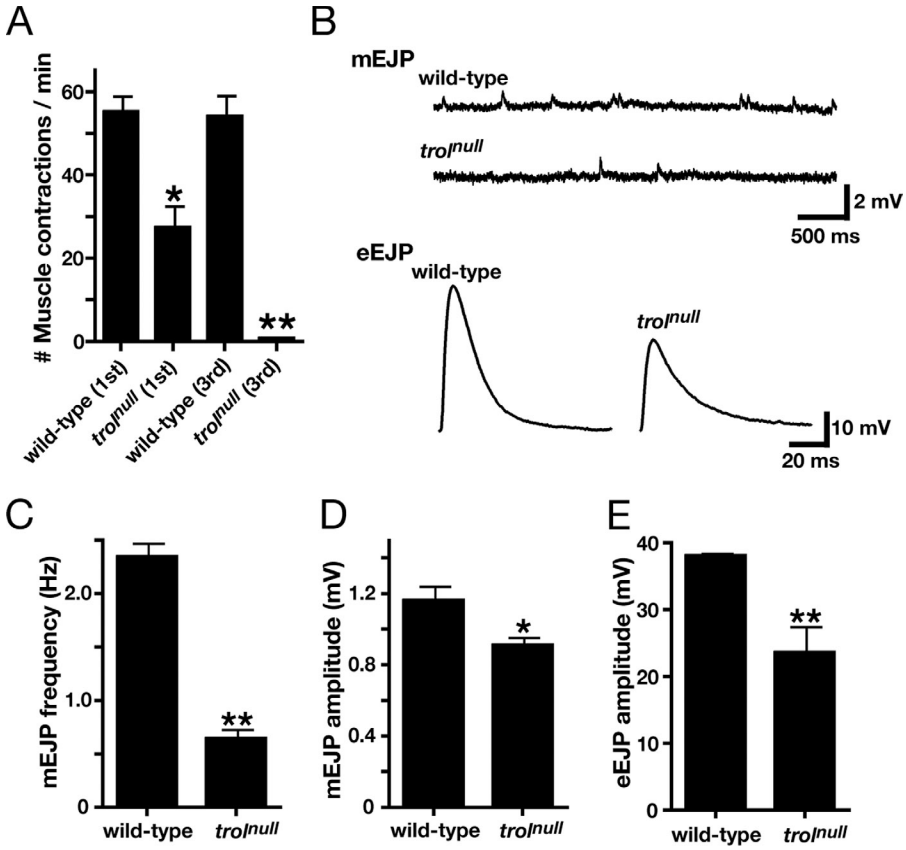

Figure 2. **Larval locomotion and electrophysiological analyses of *trol*^{null} mutants.** (A) Larval locomotion was quantified as the number of muscular body contractions per minute during crawling of first- and third-instar larvae of wild-type and *trol*^{null} mutants. (B) Representative traces of mEJP and eEJP showed that *trol*^{null} mutants had defective synaptic transmission. (C–E) *trol*^{null} mutants displayed decreased frequency (C) and amplitude (D) of mEJP and decreased eEJP amplitude (E). Error bars represent SEM (*, $P < 0.05$ and **, $P < 0.005$ relative to wild type). Sample numbers: (A) $n = 10$; (C–E) $n = 11$.

modulate Wnt/Wg signaling by regulating Wnt/Wg distribution in the synapses. To test this possibility, we examined the *Drosophila* NMJs of various mutants for HSPG-related genes and found that mutations in *terribly reduced optic lobes* (*trol*), encoding a secreted HSPG, perlecan, resulted in the characteristic abnormalities in the NMJ that were reminiscent of the phenotypes of Wg pathway mutants. Here, we show that, in the *trol* mutants, the presynaptic canonical Wg pathway was enhanced, whereas the postsynaptic FNI pathway was suppressed, presumably by the disrupted transport of Wg in the NMJ synapses. Thus, we suggest that Trol is required to distribute Wg proteins precisely in developing NMJ synapses, balancing the pre- and postsynaptic activities of Wg signaling. To our knowledge, this is a first study to demonstrate that HSPG contributes to the short-range bidirectional signal control of Wnt at synapses.

Results

Trol is required for functional NMJ formation

In vertebrates, two HSPGs, agrin and perlecan, play pivotal roles in NMJ formation (Singhal and Martin, 2011). Although no obvious orthologues of agrin have been identified in *Drosophila*, there is a single fly perlecan gene named *trol* (Voigt et al., 2002). To clarify the Trol function, null and hypomorphic alleles of *trol* mutants were used, *trol*^{null} and *trol*^{7}, which lack the entire coding region and the C terminus, respectively (Voigt et al., 2002; Park et al., 2003). We examined the morphology of larval NMJs located on muscle 6/7 by immunohistochemistry with antibodies against HRP (presynaptic marker) and Discs large (DLG), a *Drosophila* homologue of the mammalian PSD-95 (postsynaptic marker). In wild-type, synaptic boutons increased in number during larval development concomitant with the increase in muscle size (Fig. 1, A, E, and F; Schuster et al., 1996). We first noticed that muscle size was reduced in *trol*^{null} and *trol*^{7} mutants (Fig. 1 E). Growth defect of *trol* muscles was first detected at the second-instar larval stage and became pronounced at the third-instar stage, indicating that Trol is required for muscle growth. Furthermore, we observed that the subsets of synaptic boutons in *trol* mutants lacked postsynaptic DLG (Fig. 1, B, C, and G). These boutons are called "ghost boutons," which have been identified in several Wg signaling mutants (Packard et al., 2002; Ataman et al., 2006; Mosca and Schwarz, 2010). The ghost boutons in *trol* mutants appeared as early as the first-instar larval stage. In addition to the postsynaptic defects, *trol* mutants showed overproduction of small synaptic boutons formed on the short branches that project from the main shaft of the NMJ (satellite boutons; Fig. 1, D and H). Although the muscles in *trol* mutants were remarkably small compared with those in wild-type animals, the total number of synaptic boutons in these mutants was comparable to that in the wild type owing to the presence of satellite boutons (Fig. 1 F).

Consistent with these morphological defects of the NMJ, the *trol*^{null} mutant larvae showed abnormality in crawling behavior. We counted the number of peristaltic contractions

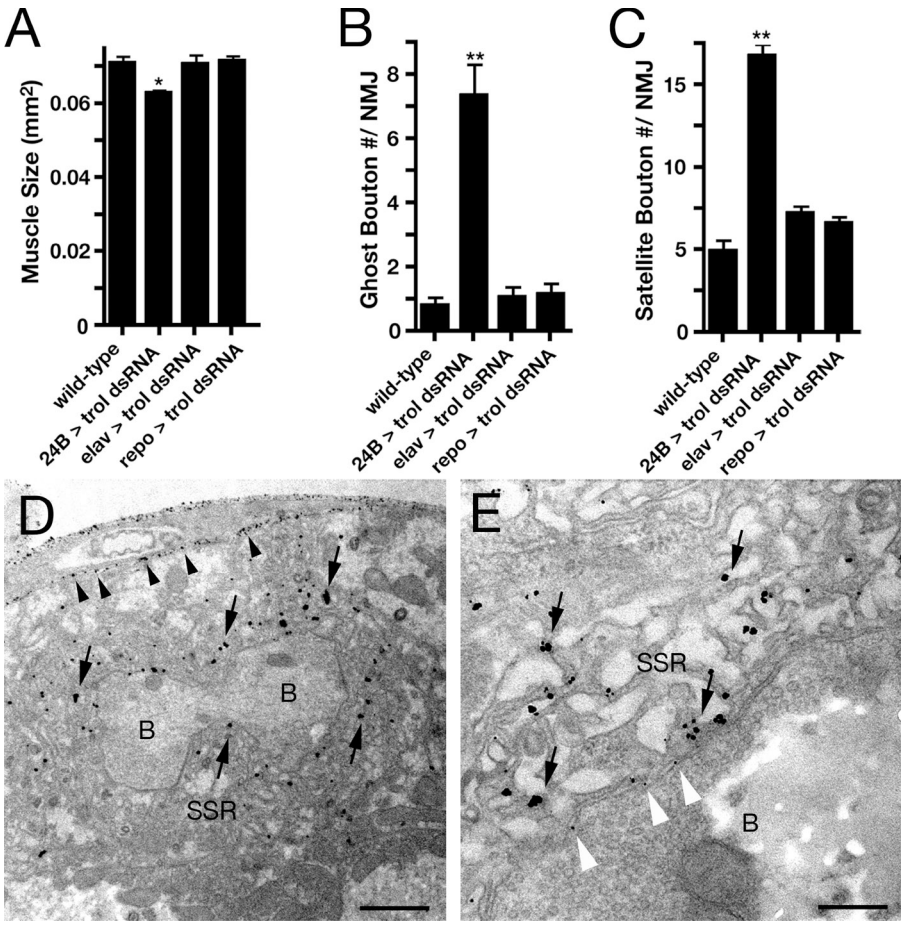

Figure 3. **Trol is localized at postsynaptic SSR and functions postsynaptically.** (A–C) Area of muscle 6/7 (A) and the numbers of ghost (B) and satellite boutons (C) in the NMJs of *24B>trol dsRNA*, *elav>trol dsRNA*, and *repo>trol dsRNA* animals, in which Trol was knocked down specifically in muscle, neuron, and glia, respectively, were quantified. Muscle-specific *trol* knockdown caused reduction of muscle area and increase of ghost and satellite boutons. Error bars represent SEM ($n = 20$; *, $P < 0.01$ and **, $P < 0.001$ relative to wild type). (D and E) Immunoelectron microscopy was performed for the synaptic bouton regions of the *trol* FlyTrap line. Localization of Trol was analyzed by immunostaining with the anti-GFP antibody. Arrows indicate Trol signals in the SSR. (E) White arrowheads indicate the localization of Trol signals at the perisynaptic region between pre- and postsynaptic membranes. (D) Trol signals were also detected on basement membranes (black arrowheads). Bars: (D) 1 µm; (E) 300 nm. B, synaptic bouton.

while larvae crawled on an agar plate (Fig. 2 A). Notably, although the first-instar larvae of $trol^{null}$ mutants have normal-sized muscles, these animals showed a significantly reduced number of contractions per minute. The locomotion defects of $trol^{null}$ animals were more obvious at the third-instar larval stage, at which point they stayed at the same position during our assay period without muscle contraction.

We next analyzed the electrophysiological properties of muscle 6 of $trol^{null}$ mutant larvae (Fig. 2, B–E). In the $trol^{null}$ mutants, the frequency of spontaneous miniature excitatory junction potentials (mEJPs) was remarkably decreased (Fig. 2, B and C), suggesting reduction of the probability of spontaneous vesicle release in the motor neuron axon terminals and/or the dysfunction of postsynaptic glutamate receptors. In addition, amplitudes of the mEJP and the evoked excitatory junction potential (eEJP) induced by nerve stimulation were also decreased (Fig. 2, B, D, and E). The quantal contents, the numbers of synaptic vesicles released with each stimulus, were not significantly different between wild-type and $trol^{null}$ animals (28.2 ± 6.4 compared with 37.2 ± 3.1 for wild type; $P = 0.16$), suggesting that the presynaptic neurotransmitter release machinery was not severely disrupted. These results suggested that postsynaptic responses were decreased in the NMJ of $trol^{null}$ mutant larvae, leading to their locomotion defects. However, we cannot exclude the possibility that the locomotion defects were also caused by abnormalities in the CNS of the $trol^{null}$ mutant.

Trol is localized at postsynaptic subsynaptic reticulum (SSR)

To examine where Trol functions at the larval NMJ, we used transgenic RNAi, a conditional knockdown system in *Drosophila* (Dietzl et al., 2007). We expressed double-stranded hairpin RNA (dsRNA) of *trol* specifically in muscle, neuron, and glia using the upstream activation sequence (UAS)/Gal4 system. As shown in Fig. 3, muscle-specific expression of *trol* dsRNA (*24B>trol dsRNA*) reduced the muscle size and increased the numbers of satellite and ghost boutons, which were markedly similar to the *trol* mutant phenotype. On the other hand, neither neuronal (*elav>trol dsRNA*)- nor glial (*repo>trol dsRNA*)-specific *trol* RNAi affected the formation of both muscles and synaptic boutons (Fig. 3, A–C). Thus, it was suggested that muscle-derived Trol contributes to muscle growth and NMJ formation.

Next, to determine the subcellular localization of Trol at NMJ, we performed immunoelectron microscopic analyses (Fig. 3, D and E) using the FlyTrap transgenic fly line, ZCL1700, which expresses the Trol-GFP fusion protein under an endogenous promoter (Guha et al., 2009). We stained the *trol* FlyTrap larvae with the anti-GFP antibody using the preembedding nanogold silver intensification technique. Consistent with a previous study, immunogold signals were found to be localized at the basement membrane of various tissues, including muscle cells (Fig. 3 D, arrowheads; Friedrich et al., 2000). Many immunogold signals were observed in association

with the SSR, highly convoluted folds of the postsynaptic muscle plasma membranes (Fig. 3, D and E, arrows). The positive signals were also observed in the extracellular space between pre- and postsynaptic membranes (Fig. 3 E, arrowheads). Thus, it was suggested that Trol is secreted by the muscle cells and is accumulated mainly in the SSR membrane at the NMJ.

Both the core protein and HS moieties of Trol contribute to NMJ development

Perlecan regulates diverse signaling pathways by binding to many proteins through both the core protein and HS chains (Whitelock et al., 2008). So, we next tried to get information regarding the parts of Trol that contribute to NMJ formation. During biosynthesis of HS, the enzyme encoded by *sulfateless* (*sfl*), a homologue of mammalian *glucosaminyl N-deacetylase-N-sulfotransferase*, initiates the polysaccharide modifications by generating *N*-sulfate groups (Maeda et al., 2011). Because *N*-sulfation is a prerequisite for the subsequent HS modifications, defects in *sfl* lead to generation of undersulfated polysaccharides, which would show reduced affinity for most HS-binding proteins (Toyoda et al., 2000).

Thus, we knocked down *sfl* specifically in muscles and examined its effects on *trol* mutations. Muscle-specific expression of *sfl* dsRNA (*24B>sfl dsRNA*) in wild-type animals significantly reduced the muscle size, suggesting that HS plays important roles in muscle growth (Fig. 4 G). However, the same manipulation did not affect the muscle size of $trol^{null}$ mutants ($trol^{null}$*; 24B>sfl dsRNA*). This suggested that HS chains attached to the core proteins other than that of Trol play minor roles in muscle growth. Muscle-specific expression of the secreted form of Dally, a *Drosophila* glycosylphosphatidylinositol-anchored HSPG, glypican, did not rescue the muscle phenotype of $trol^{null}$ mutants ($trol^{null}$*; 24B>sec-dally*), supporting the importance of Trol core protein and its HS modifications (Fig. 4 G). The ghost bouton phenotype of $trol^{null}$ mutants was augmented by muscle-specific expression of *sfl* dsRNA, although the difference was not statistically significant (Fig. 4, E and H). This might be interpreted that HS chains on the core proteins other than that of Trol suppressed the ghost bouton phenotype of $trol^{null}$ mutants. We found consistently that muscle-specific expression of *sec-dally* rescued the ghost bouton phenotype of $trol^{null}$ mutants, suggesting that HS chains rather than specific core protein portions might be important for this phenotype (Fig. 4, F and H). On the other hand, neither *sfl* dsRNA nor *sec-dally* affected the satellite bouton phenotype of $trol^{null}$ mutants, suggesting that this phenotype is mainly dependent on the core protein portion of Trol (Fig. 4 I).

trol mutants show diverse postsynaptic defects

We analyzed the morphology of $trol^{null}$ NMJ using transmission electron microscopy (Fig. 5, A–I). As reported previously, the basement membrane of $trol^{null}$ mutant was closely apposed to the muscle cell surface compared with the wild type, but the overall structure of muscles appeared to be normal in this mutant (Fig. 5, A and B; Pastor-Pareja and Xu, 2011). However, mutations in *trol* caused severe structural defects in the NMJ. We found that the area of postsynaptic SSR was dramatically reduced in $trol^{null}$ mutants (Fig. 5, C, D, and G). The SSR of wild-type animals appeared as complex alternating layers of clear extracellular and opaque intracellular spaces (Fig. 5, C and E). In the $trol^{null}$ mutants, the SSR layers were densely packed, and the number of layers was also decreased, leading to the small SSR phenotype (Fig. 5, D and F). In contrast to the drastic changes in the postsynaptic structure, many parameters of presynaptic terminals, such as the density of synaptic vesicles (Fig. 5 I) and the number of mitochondria ($0.12 \pm 0.01/\mu m^2$ compared with $0.10 \pm 0.02/\mu m^2$ for wild type; $P = 0.46$), were normal in the $trol^{null}$ mutants. However, the size of presynaptic boutons appeared to be slightly reduced because of the presence of small satellite boutons ($2.4 \pm 0.2\ \mu m^2$ compared with $2.7 \pm 0.1\ \mu m^2$ for wild type; $P = 0.21$), although the difference was not statistically significant.

Next, we analyzed the active zones, the electron-dense thickening of presynaptic membranes, and the T bar, T-shaped electron-dense projections (Fig. 5, E and F, arrowheads). The number of active zones ($0.09 \pm 0.01/\mu m^2$ compared with $0.11 \pm 0.02/\mu m^2$ for wild type; $P = 0.08$) and the morphology of T bar were normal in $trol^{null}$ mutants; however, the postsynaptic area immediately apposed to the active zones was remarkably altered. Although this postsynaptic area contained a shallow pocket of amorphous materials in the wild-type animals, this pocket was dramatically enlarged in the $trol^{null}$ mutants (Fig. 5, E, F, and H).

We next immunohistochemically stained the larval NMJ using antibodies against a subunit of glutamate receptor (GluRIIA) and Bruchpilot (BRP), an active zone marker. In the wild type, GluRIIA signals were localized at the postsynaptic sites apposed to the BRP signals (Fig. 5 J). In the $trol^{null}$ mutants, the intensity of GluRIIA signals was dramatically reduced in the majority of boutons (Fig. 5, K and L). On the other hand, the number and intensity of BRP signals were not affected (Fig. 5 L), consistent with the aforementioned ultrastructural experiments, indicating that the number and morphology of active zones were normal in the $trol^{null}$ mutants. Thus, our analyses revealed the diverse postsynaptic defects in the NMJ of $trol^{null}$ mutants and suggested that the defects in the synaptic transmission were caused mainly by these postsynaptic dysfunctions.

Trol promotes the FNI pathway of Wg signaling during postsynaptic development

It has been revealed that *wg* loss-of-function mutations lead to diverse pre- and postsynaptic defects at larval NMJ, including decreases in the number of active zones and the SSR area, increases in the enlarged postsynaptic pockets and the ghost boutons, and altered active zone structure and GluRIIA distribution (Packard et al., 2002). Because the defects in the postsynaptic structure of *trol* mutants were extremely similar to those of *wg* loss-of-function mutants, we examined whether Trol regulates the activity of Wg signaling during postsynaptic development (Fig. 6). Previous studies indicated that presynaptically released Wg activates the postsynaptic DFz2, leading to the cleavage of the C terminus of the receptor (DFz2-C), which is translocated

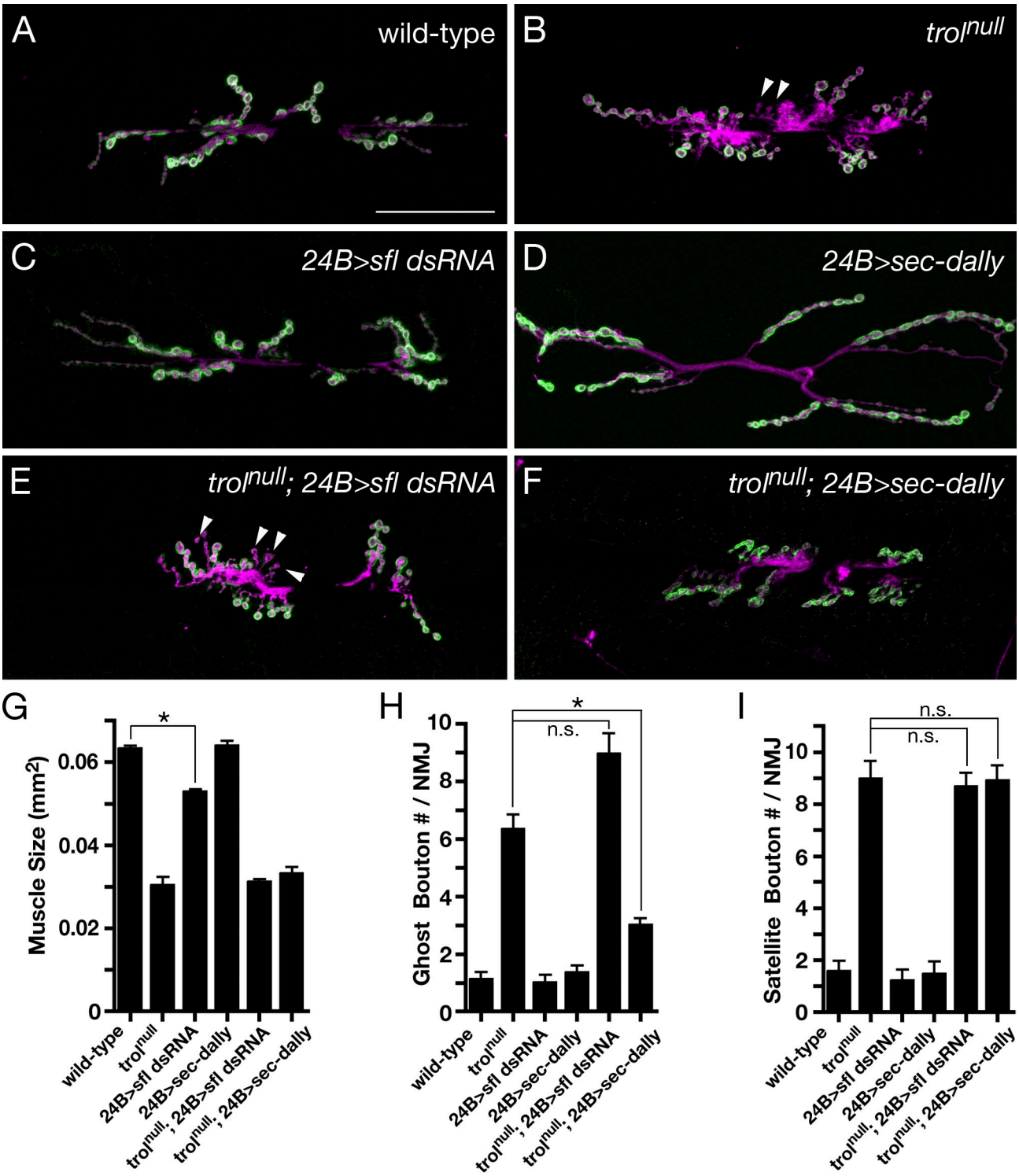

Figure 4. **Both the core protein and HS moieties of Trol are required for NMJ formation.** (A–F) Larval NMJs of wild type (A), *trol*^{null} (B), *24B>sfl dsRNA* (C), *24B>sec-dally* (D), *trol*^{null}*; 24B>sfl dsRNA* (E), and *trol*^{null}*; 24B>sec-dally* (F) were stained with anti-HRP (magenta) and anti-DLG (green) antibodies. Arrowheads in B and E indicate ghost boutons. Bars, 50 µm. (G–I) Area of muscle 6/7 (G) and the numbers of ghost (H) and satellite (I) boutons in animals of indicated genotypes were measured. Muscle-specific expression of *sfl dsRNA* reduced muscle size (*24B>sfl dsRNA*). The ghost bouton phenotype of the *trol*^{null} mutant was rescued by muscle-specific expression of *sec-dally* (*trol*^{null}*; 24B>sec-dally*) but not by *sfl dsRNA* (*trol*^{null}*; 24B>sfl dsRNA*). Expression of neither *sfl dsRNA* nor *sec-dally* affected the satellite bouton phenotype of the *trol*^{null} mutant. Error bars represent SEM (n = 18; *, $P < 0.01$).

into muscle nuclei (Mathew et al., 2005). This FNI pathway is required for the development of the postsynaptic apparatus of the NMJ (Mosca and Schwarz, 2010). To investigate the involvement of Trol in the FNI pathway, we examined whether *trol* mutations affect the translocation of DFz2-C into muscle nuclei using the antibody against the DFz2-C. In wild type, DFz2-C signals showed a punctate pattern in the muscle nuclei (Fig. 6 A, arrowheads), in addition to robust signals at the

synaptic boutons (Fig. 6 A, arrow). We found that *trol*^{null} mutations dramatically reduced the DFz2-C signals in the muscle nuclei without affecting their localization at the synaptic boutons (Fig. 6, B and C), suggesting that Trol is required for the activation of Wg signaling in the postsynaptic cells.

We next investigated whether the postsynaptic defects of *trol* mutants arise from the reduced activities of Wg signaling. We restored the FNI pathway of Wg signaling in the *trol*^{null} muscles by expressing the C terminus of DFz2 fused to an NLS (*DFz2-C–NLS*; Mosca and Schwarz, 2010). We investigated four parameters related to NMJ development: number of ghost boutons, SSR structures, number of enlarged postsynaptic pockets, and localization of GluRIIA (Fig. 6, D–J). As shown in Fig. 6 G, the expression of *DFz2-C–NLS* transgene in *trol*^{null} muscles (*trol*^{null}*; 24B>DFz2-C–NLS*) reduced the number of ghost boutons to the wild-type level. Furthermore, *DFz2-C–NLS* expression significantly rescued the phenotypes of small SSR and the postsynaptic enlarged pockets around active zones in *trol*^{null} mutants (Fig. 6, F, H, and I). These results provide strong evidence that the defects of postsynaptic structure in *trol* mutants arose from the reduced activity of Wg signaling in the muscles.

Although the small SSR area of *trol* mutants was significantly restored by the *DFz2-C–NLS* expression, the thickness of each SSR layer remained thin in these transgenic animals (Fig. 6 F). In particular, it is noteworthy that the amounts of extracellular space around folds remained small in these animals. Furthermore, the expression of *DFz2-C–NLS* did not rescue the defects of GluRIIA localization and electrophysiological properties of *trol*^{null} NMJ (Fig. 6 J and Fig. S1). Mosca and Schwartz (2010) have shown that *importin-β11/α2* is required for the translocation of DFz2 to the muscle nuclei, but its mutation did not affect the localization of GluRIIA at NMJ, suggesting that Wg regulates the GluRIIA localization by an FNI-independent pathway. It is thus considered that Trol controls the GluRIIA localization and so controls synaptic transmission by the Wg signaling that is independent of the FNI pathway or by another signaling pathway unrelated to Wg. Finally, the GluRIIA localization does not seem to be critically dependent on the sulfation of HS because the NMJs of *sft*^{null} mutants showed normal levels of GluRIIA expression (Fig. S2).

Satellite bouton phenotype of *trol* mutants is suppressed by reduced Wg signaling

The ultrastructural organization of presynaptic terminals, such as the number and morphology of active zones, was apparently normal in *trol* mutants, which was a marked contrast to the *wg* loss-of-function mutants showing various presynaptic defects in addition to the postsynaptic ones (Packard et al., 2002). Instead, *trol* mutants showed the overproduction of type I synaptic boutons (Fig. 7 D). It is noteworthy that this increase of satellite boutons in *trol* mutants was not caused by the reduced FNI signaling in the postsynaptic cells because expression of *DFz2-C–NLS* in *trol*^{null} muscles did not rescue their satellite bouton phenotype (Fig. 7 A). Recent studies have shown that the satellite boutons are induced by the excess signaling activities of Wg and/or Glass bottom boat (Gbb), a *Drosophila* homologue of bone morphogenetic protein (BMP; Packard et al., 2002; Miech et al., 2008; O'Connor-Giles et al., 2008). Thus, to examine the possibility that *trol* mutations up-regulate the presynaptic activities of Wg and/or Gbb, we investigated whether mutations in these signaling pathways affect the satellite bouton phenotype of *trol* mutants (Fig. 7, B–F). The heterozygous mutations of *wg* significantly suppressed the satellite bouton phenotype of *trol*^{null} animals (*trol*^{null}*; wg*^{CX4}/+; Fig. 7, B and E). This effect was specific to the *wg* mutations because the heterozygous mutation of *gbb* did not show similar effects (*trol*^{null}*; gbb*^{1}/+; Fig. 7, B and F). We additionally studied the contribution of FGF receptor Heartless, which is essential for muscle development (Shishido et al., 1997). As shown in Fig. S3, the heterozygous mutations of *heartless* (*htl*^{AB42}/+) did not affect the ghost and satellite bouton phenotypes of *trol* mutants.

To examine whether presynaptic canonical Wg signaling was increased in the *trol* mutants, we next tried to reduce its activity specifically in the motor neurons. *sgg* and *dsh* are negative and positive regulators of the canonical Wg signaling, respectively (Axelrod et al., 1998; Bourouis, 2002; Miech et al., 2008), and thus, we expressed the active form of *sgg* and the dominant-negative form of *dsh* in *trol*^{null} motor neurons using *OK6-Gal4* driver (*trol*^{null}*; OK6>sgg*^{act} and *trol*^{null}*; OK6>dsh*^{DIX}, respectively). These manipulations completely suppressed the satellite bouton phenotype of *trol*^{nul} mutants (Fig. 7, B, G, and H), although the ghost bouton phenotype was not rescued (Fig. 7, G and H, arrowheads). These results suggested that the canonical Wg signaling was elevated in the presynaptic motor neurons of *trol* mutants.

Previous studies have shown that Wg signaling regulates the cytoskeletal organization in presynaptic terminals (Packard et al., 2002; Miech et al., 2008). During NMJ development, Futsch, a microtubule-associated protein, associates with loops of bundled microtubules within subsets of boutons. This Futsch loop is essential for synaptic growth, and its formation is promoted by activation of Wg signaling (Miech et al., 2008). As expected, we found that the number of Futsch loops was increased in the NMJ of *trol*^{null} mutants (Fig. 7, I–K), suggesting that Trol suppresses the presynaptic activity of Wg signaling during NMJ formation.

Trol regulates the extracellular distribution of Wg

We next expressed the Wg-GFP fusion protein in the motor neurons of *trol*^{null} mutants and investigated the extracellular levels of Wg-GFP at the NMJ using an extracellular staining protocol (Strigini and Cohen, 2000). In wild type, the extracellular Wg was diffusely distributed at the surroundings of presynaptic terminals (Fig. 8, A, D, and F). At the *trol*^{null} boutons, the extracellular levels of Wg were significantly reduced without affecting the total Wg-GFP level, indicating that Trol regulates the extracellular localization of Wg at NMJ (Fig. 8, B, C, E, and F). Detailed analyses of Wg localization at the single bouton level showed that the extracellular Wg did not spread and was deposited closely around the presynaptic membranes in *trol*^{null} mutants (Fig. 8, D–F). This finding suggested that Trol regulates

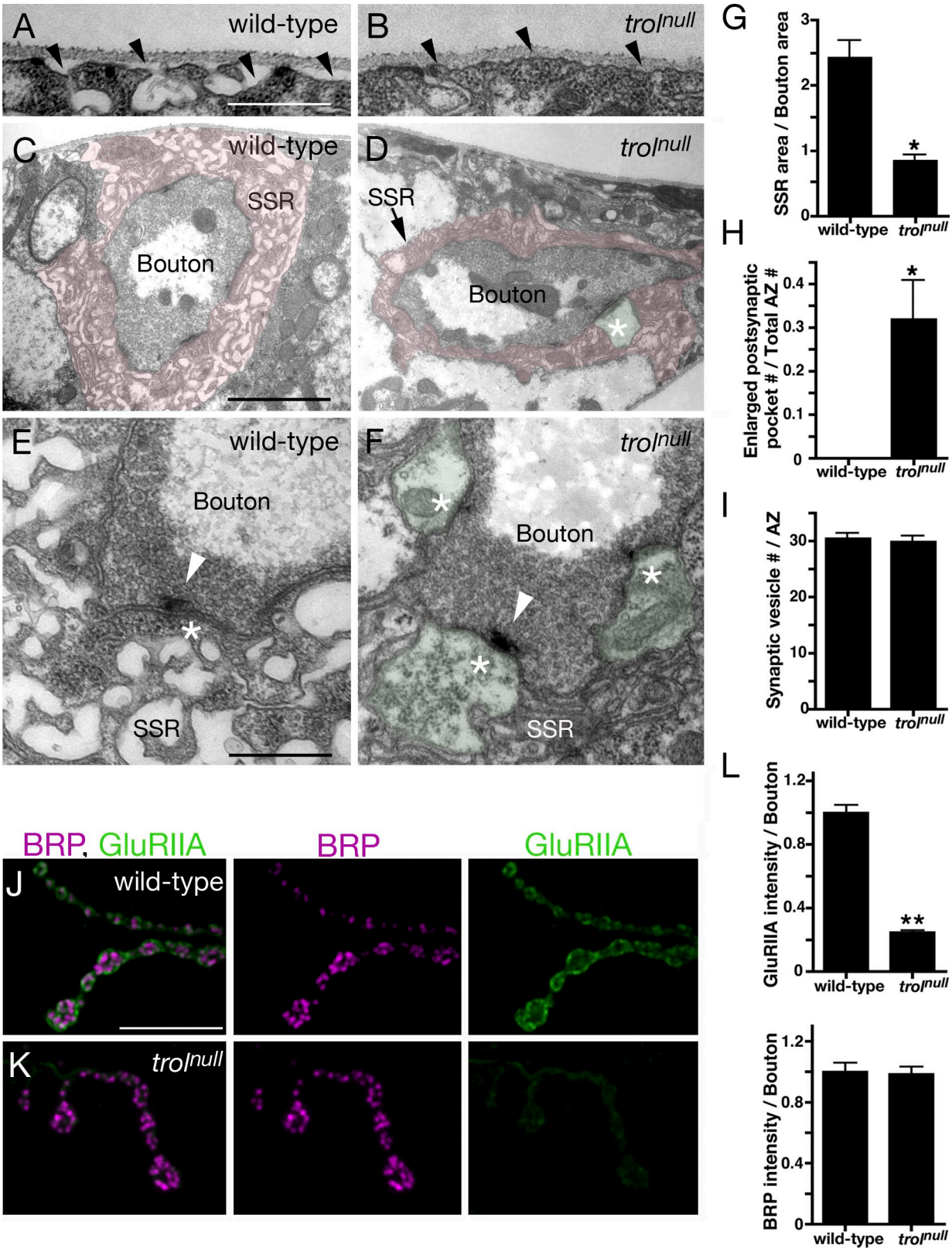

Figure 5. **Trol is required for formation of postsynaptic structures and glutamate receptor localization at postsynaptic sites.** (A–F) Electron micrographs of wild-type (A, C, and E) and *trol*^{null} mutant (B, D, and F) tissues are presented. In *trol*^{null} mutants, the cell surface of muscle is located closer to the basement membrane (arrowheads in B) than in the wild type (A). Mutations in *trol* caused small SSRs (D) and abnormally enlarged pockets in the postsynaptic region apposed to active zones (asterisks in D and F). The structure of T bar appeared normal in the *trol*^{null} mutant (arrowheads in E and F). Arrowheads in A indicate the cell surface of the muscle. An asterisk in E indicates the normal postsynaptic area apposed to the active zone. (G–I) Morphometric analyses of type Ib boutons showed that the SSR area was decreased (G), and the number of enlarged pockets increased (H) in *trol*^{null} mutants. On the other hand, the number of synaptic vesicles was not altered in *trol*^{null} mutants (I). To count the number of synaptic vesicles, we selected those within 250 nm of the active

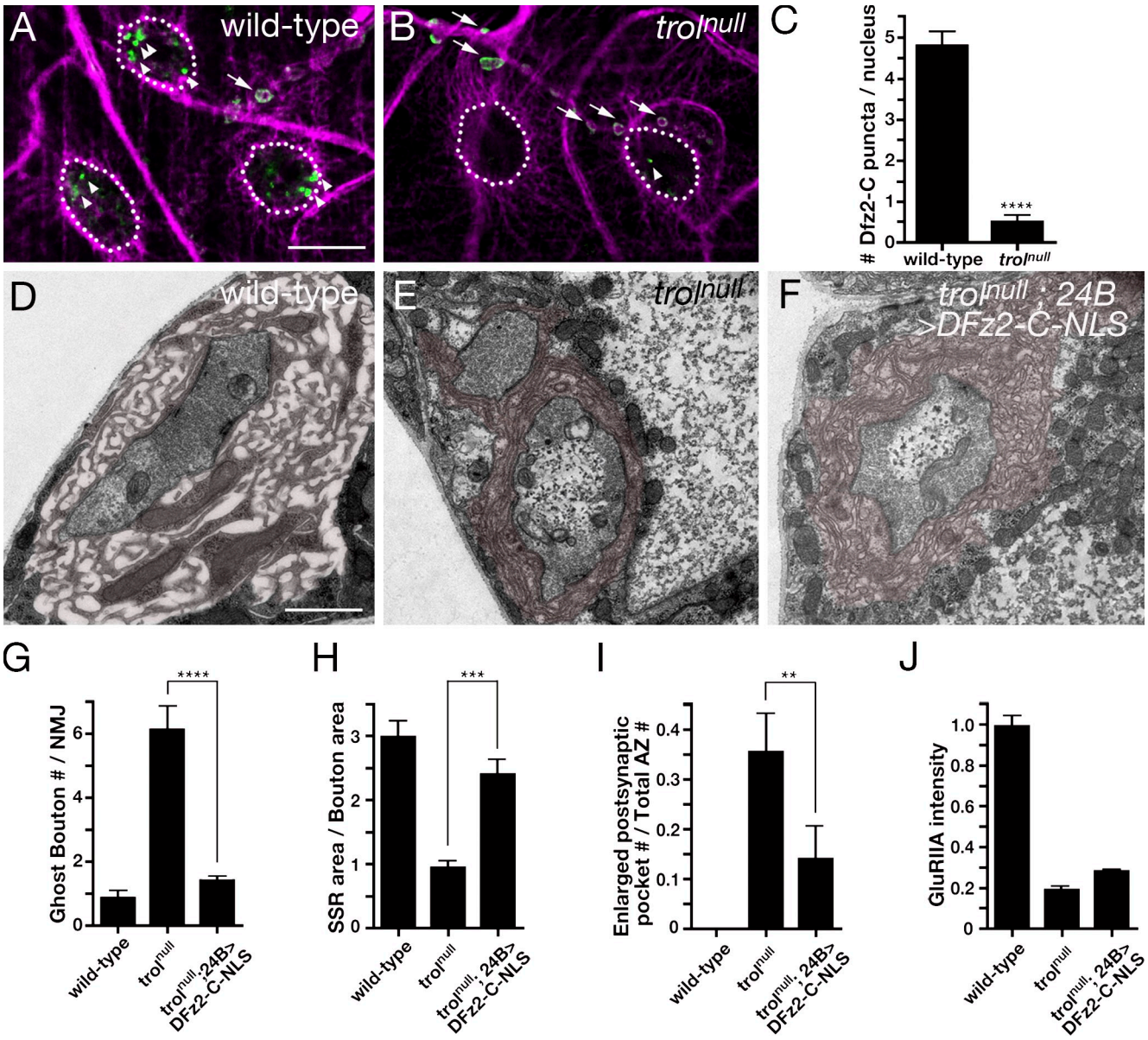

Figure 6. **Trol regulates Wg-mediated postsynaptic development.** (A–C) Muscle 6 in wild-type (A) and *trol*^{null} (B) animals was stained with antibodies to the C terminus of Dfz2 (green) and α-Tubulin (magenta). Immunoreactive puncta in the nuclei (arrowheads in dashed circles) were markedly reduced in *trol*^{null} mutants. DFz2-C localization in the synaptic boutons was not affected by mutations in *trol* (arrows). (C) The numbers of DFz2-C nuclear puncta in third-instar larval muscles of wild-type and *trol*^{null} animals were counted. (D–F) Electron micrographs of synaptic type I boutons of wild-type (D), *trol*^{null} (E), and *trol*^{null}*; 24B>DFz2-C–NLS* (F) animals are presented. The SSR region is colored brown. (G–J) Expression of *DFz2-C–NLS* in *trol*^{null} muscles rescued their ghost bouton (G), small SSR (H), and enlarged postsynaptic pocket (I) phenotypes. However, *DFz2-C–NLS* expression did not rescue the abnormal localization of GluRIIA at *trol*^{null} synaptic boutons (J). Error bars represent SEM (n = 20; **, $P < 0.01$; ***, $P < 0.001$; and ****, $P < 0.0001$). Bars: (A) 15 µm; (D) 1 µm. AZ, active zone.

the trafficking of Wg from presynaptic terminals to the postsynaptic membrane.

A previous study has indicated that HSPGs bind to Wnt via HS chains (Reichsman et al., 1996). To directly examine whether HS regulates the localization of Wg at the NMJ, we degraded HS with heparitinase and evaluated its effects on the extracellular Wg distribution at NMJs (Fig. 8, G–I). About 60% of HS was degraded after heparitinase treatment as judged by the staining intensity of 10E4 anti-HS monoclonal antibody (Fig. S4). Under this condition, the extracellular Wg levels on

zones. Error bars represent SEM (n = 15; *, $P < 0.0001$). (J–L) Synaptic regions of wild-type (J) and *trol*^{null} mutants (K) were stained with the antibodies against active zone marker BRP and GluRIIA. (J) BRP and GluRIIA clusters were located on apposed membranes at the synaptic boutons in wild-type larvae. (K) In *trol*^{null} mutants, the levels of GluRIIA, but not BRP, were dramatically decreased compared with those of wild-type animals. (L) Bar graphs show the mean staining intensity for GluRIIA and BRP at the NMJ. Error bars represent SEM (n = 20; **, $P < 0.001$). Bars: (A, B, E, and F) 500 nm; (C and D) 1.5 µm; (J and K) 15 µm. AZ, active zone.

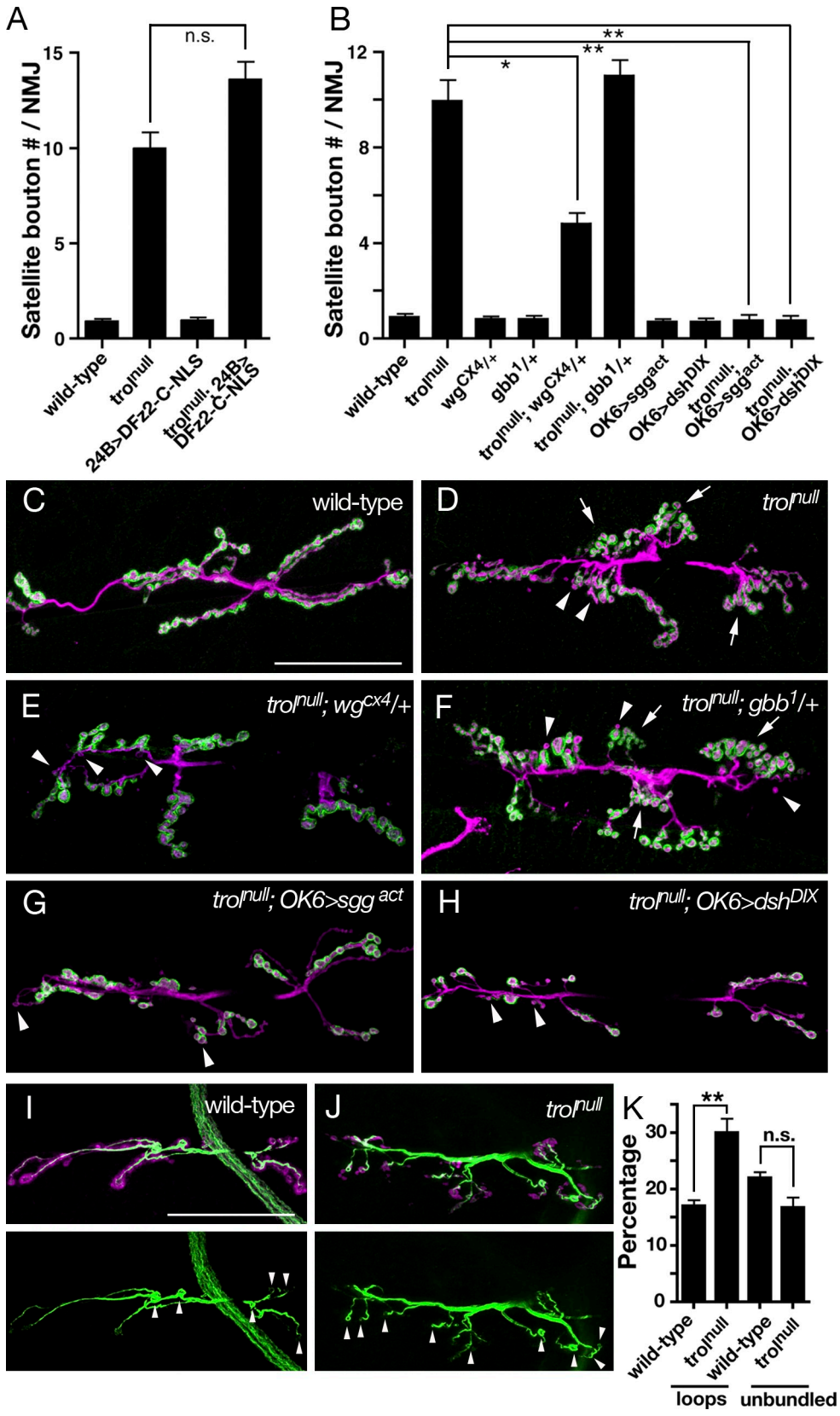

Figure 7. **Reduction of presynaptic Wg signaling suppresses satellite bouton phenotype of *trol* mutants.** (A) Activation of FNI pathway in the muscles (*trol*^{null}; *24B>DFz2-C–NLS*) did not rescue the satellite bouton phenotype of *trol*^{null} mutants. (B–H) The numbers of satellite boutons in muscle 6/7 of the indicated genotypes were counted (B). Larval NMJs of wild type (C), *trol*^{null} (D), *trol*^{null}; *wg*^{CX4}/+ (E), *trol*^{null}; *gbb*^{1}/+ (F), *trol*^{null}; *OK6>sgg*^{act} (G), and *trol*^{null}; *OK6>dsh*^{DIX} (H) were stained with anti-HRP (magenta) and anti-DLG (green) antibodies. Heterozygous mutation of *wg* (E), but not that of *gbb* (F), suppressed the satellite bouton phenotype of *trol*^{null} animals (B). Presynaptic suppression of canonical Wg signaling (G and H) rescued the satellite bouton phenotype (B), but not the ghost bouton phenotype, of *trol*^{null} animals. Arrows and arrowheads indicate the satellite and ghost boutons, respectively. (I–K) The NMJs of wild-type (I)

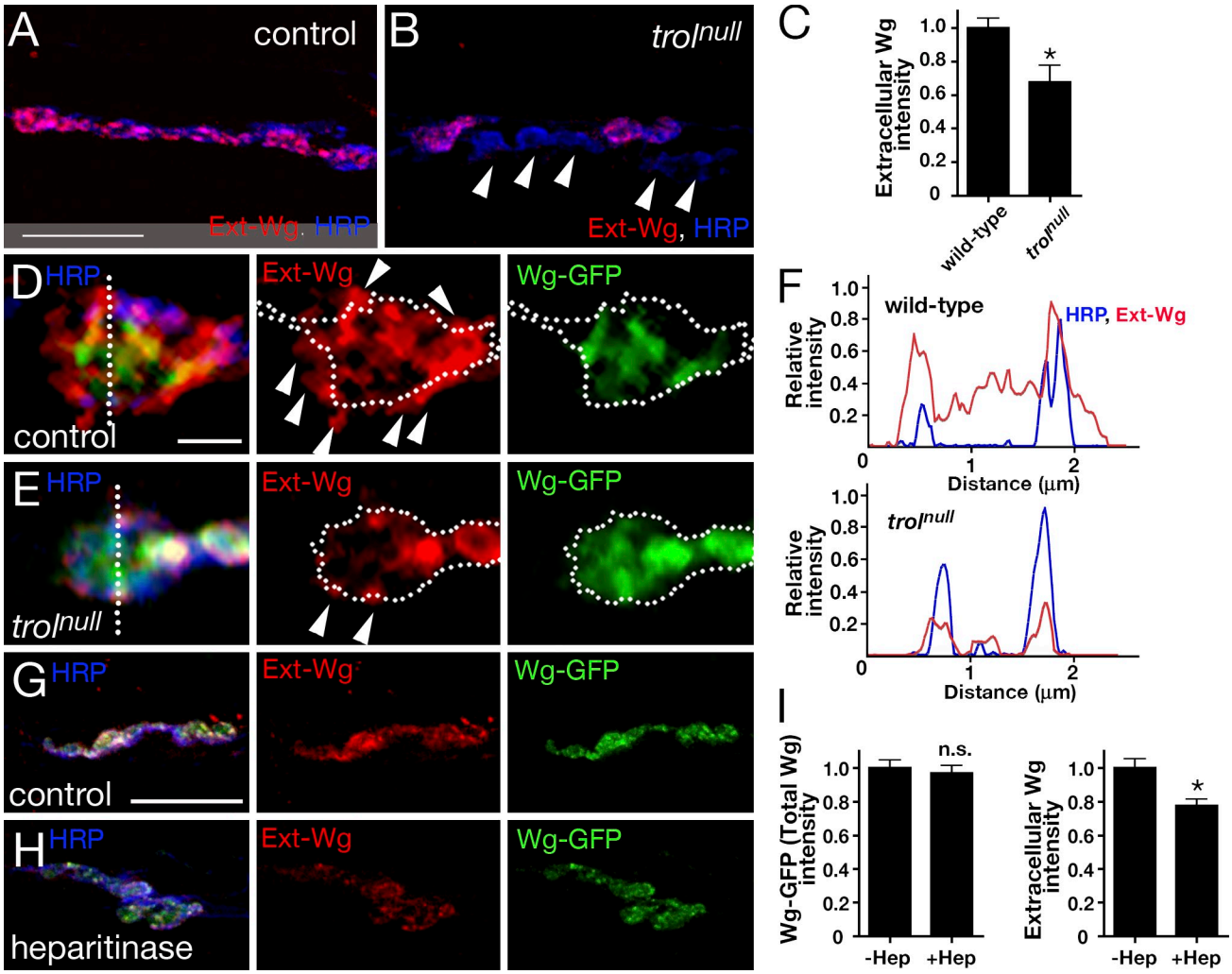

Figure 8. **Trol regulates the extracellular distribution of Wg.** (A–F) The NMJs of *OK6>GFP-wg* (A and D) and *trol*^{null}*; OK6>GFP-wg* (B and E) larvae, which expressed Wg-GFP specifically in the motor neurons, were stained using a protocol detecting extracellular Wg (Ext-Wg). The immunostainings of presynaptic membrane (HRP) and total Wg-GFP are also shown. The majority of the *trol*^{null} boutons showed greatly reduced levels of extracellular Wg-GFP protein (arrowheads in B) compared with the wild type (A). (C) Bar graph shows the mean staining intensity of extracellular Wg-GFP at the NMJ. (D) In the wild type, extracellular Wg-GFP proteins were diffusely spread into the postsynaptic region (arrowheads). (E) In the *trol*^{null} boutons, extracellular Wg-GFP proteins were closely associated with the presynaptic membranes with little spreading into postsynaptic regions (arrowheads). Dotted curved lines trace the outlines of presynaptic terminals. (F) Plot profiles of the intensities of HRP and extracellular Wg labeling along a line crossing a bouton of wild type and *trol*^{null} are shown. The data shown are from a single representative experiment out of three repeats (n = 13). (G–I) *OK6>GFP-wg* larval NMJs were incubated with (H) or without (G) heparitinase I followed by extracellular staining of Wg-GFP. Removal of HS did not affect the total levels of Wg-GFP but significantly reduced the extracellular levels of Wg-GFP. (I) Bar graphs show the mean staining intensities of total (left) and extracellular Wg-GFP (right) levels at the NMJ. Hep, heparitinase. Error bars represent SEM (n = 25; *, $P < 0.05$). Bars: (A and G) 10 μm; (D) 1 μm.

the synaptic boutons were decreased by ~20%, although total Wg levels were not altered, suggesting that HS plays an important role in Wg localization at NMJ.

Discussion

During larval development of *Drosophila*, the muscle fibers grow rapidly; therefore, coordinated synapse formation is required to achieve proper levels of muscle depolarization. Our analyses showed that, in the NMJ of *trol* mutants, canonical Wg signaling was increased in the presynaptic motor neurons, producing satellite boutons. In contrast, the activity of the FNI Wg pathway was decreased in the postsynaptic muscle cells, which led to the abnormal postsynaptic structures. These results indicated that the balance of Wg signaling between pre- and postsynaptic compartments was disturbed in the *trol* NMJ.

We observed that Wg was localized around the presynaptic membranes and did not diffuse into the SSR regions in

and *trol*^{null} (J) animals were stained with anti-HRP (magenta) and anti-Futsch (green) antibodies. (K) Bar graph shows the percentage of boutons with Futsch loops and with unbundled Futsch in wild-type and *trol*^{null} animals. In the NMJs of *trol*^{null} mutants, synaptic boutons with Futsch loops significantly increased compared with those in wild-type animals (arrowheads in I and J). Error bars represent SEM (n = 20; *, $P < 0.05$; **, $P < 0.001$). Bars, 50 μm.

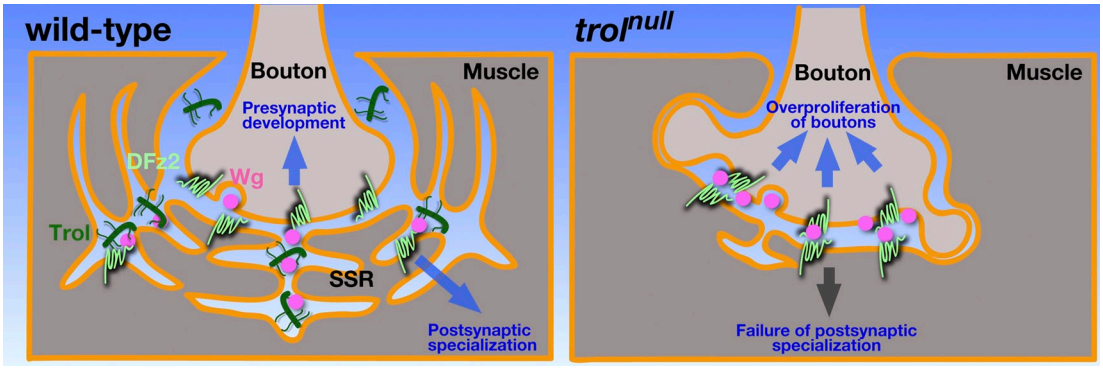

Figure 9. **Proposed model for Trol function in Wg pathway at pre- and postsynaptic cells.** In the wild type (left), presynaptically released Wg sends its signal to both presynaptic and postsynaptic cells, which is required for proliferation of boutons and formation of postsynaptic SSR, respectively. Trol binds and sequesters Wg on the surface of SSR. In *trol* mutants (right), stability of Wg at the postsynaptic site is decreased, and therefore, Wg might preferably bind its receptor DFz2 on the presynaptic membrane, inducing overproliferation of boutons. Thus, Trol regulates bidirectional activity of Wg signaling at the NMJ.

the NMJ of *trol* mutants, leading to a model in which Trol regulates the bidirectional activity of Wg by distributing the appropriate levels of Wg on both pre- and postsynaptic membranes (Fig. 9). Because Trol is highly expressed in the SSR, it is likely that Trol promotes accumulation of Wg in SSRs, which efficiently activates postsynaptic DFz2 (Fig. 9, left). In the absence of Trol, it is considered that Wg is not efficiently transported into SSRs and may be localized excessively around presynaptic boutons, leading to satellite bouton phenotype (Fig. 9, right). Our results suggested that this phenotype mainly depends on the core protein portion of Trol. In addition to the abnormal localization of Wg, the extracellular level of this protein was also significantly decreased in the NMJ of *trol* mutants, which may lead to ghost bouton phenotype. Because it is well known that HS protects many heparin-binding proteins from proteolytic degradation in the ECM (Saksela et al., 1988), this may be caused by the promoted proteolysis of Wg in the absence of Trol. In fact, we observed that at least a part of Wg bound to HS in the NMJ. These protective effects may not depend on the Trol core protein because ghost bouton phenotype of *trol* mutants was rescued by the secreted form of Dally.

Because Wg is a highly hydrophobic protein caused by acylation with palmitic acid, the diffusion and/or transport of this protein is not a simple process. Recently, it was proposed that Wg is transported from presynaptic membrane to SSR by exosome-like vesicles containing the Wnt-binding transmembrane protein Evi (Korkut et al., 2009). In this model, the exosomes carrying Wg are released from the presynaptic terminals into the synaptic clefts and are then transported to the SSR, where Wg proteins on the exosomes bind to DFz2. Importantly, Evi-containing exosomes were observed in the cisternae of SSRs (Koles et al., 2012), where immunohistochemical Trol signals were also intensely detected, suggesting the possibility that Trol supports the transport of Wg-bound exosomes in SSRs. In addition, several studies revealed that HSPGs, including perlecan, are essential for the internalization of diverse ligand molecules, such as growth factors and lipoproteins (Fuki et al., 2000; Deguchi et al., 2002). Therefore, there is a possibility that Trol directly participates in the internalization of Wg/DFz2 by muscle fibers. Further study is necessary to examine whether Trol regulates transport of exosomes as well as internalization of Wg/DFz2 in the SSR.

Besides Wg, perlecan also binds to ECM proteins, such as laminin and dystroglycan (Whitelock et al., 2008). We found that the thickness of the extracellular space of SSR layers remained thin even after Wg activation in the muscle cells of *trol* mutants, although most of the postsynaptic phenotype was rescued. This suggests that Trol is structurally required to construct ECM in the SSR, probably through interaction with these ECM components. Furthermore, Rohrbough et al. (2007) showed that mutations in *mind-the-gap* led to various abnormalities in glutamate receptor localization and postsynaptic development, which were similar to the phenotypes of *trol* mutants. Mind-the-gap is a secreted putative glycosaminoglycan-binding protein, which regulates the ECM–integrin interface at NMJ. Therefore, there is a possibility that Trol contributes to the ECM formation in coordination with Mind-the-gap, and such a precisely constructed ECM may be necessary to transport and localize Wg in the NMJ correctly. In this context, it is noteworthy that the satellite bouton phenotype of *trol* mutants mainly depends on the core protein portion of Trol. The core protein, rather than HS, may be essential for ECM construction and transport of Wg in the SSR.

Some studies on vertebrates and *Drosophila* showed that perlecan/Trol binds to various secreted molecules, such as BMP, FGF, and Hedgehog (Park et al., 2003; Lindner et al., 2007). Among these, *Drosophila* BMP orthologue Gbb expressed by muscle cells retrogradely regulates synapse growth at the NMJ (McCabe et al., 2003). *gbb* loss-of-function mutations caused reduced NMJ size, decreased neurotransmitter release, and abnormal presynaptic structure, which is a marked contrast to the phenotypes of *trol* mutants showing overgrowth of NMJ and relatively normal presynaptic structure. Because it has been revealed that HSPGs negatively regulate BMP signaling in some circumstances (Gumienny et al., 2007), presynaptic Gbb signaling might be activated without Trol. Alternatively, presynaptically expressed HSPGs may contribute to the Gbb signaling at NMJ, and postsynaptically expressed Trol may not play major roles in this signaling pathway. Our experiments indicated

that down-regulation of Gbb signaling in the *trol* mutants did not rescue the satellite bouton phenotype, supporting the latter possibility. In the *Drosophila* NMJ, syndecan and Dally-like glypican (Dlp) are expressed by pre- and postsynaptic cells, respectively (Johnson et al., 2006). It has been revealed that these HSPGs associate with DLAR, a presynaptically expressed receptor-type protein tyrosine phosphatase, and regulate synapse growth and active zone stabilization (Johnson et al., 2006). Accordingly, syndecan in the presynaptic membrane may also contribute to the Gbb signaling at NMJ. Furthermore, postsynaptically expressed Dlp may support residual Wg signaling in the *trol* mutants because it is known that this HSPG plays critical roles in the trafficking and gradient formation of Wg in *Drosophila* larval wing disc (Kirkpatrick et al., 2004; Kreuger et al., 2004).

The frequency of mEJP and the amplitude of eEJP were significantly reduced in *trol* mutants. Mutations in *sfl* and *tout-velu*, which encodes a *Drosophila* homologue of HS polymerase, EXT1, also reduced mEJP frequency (Ren et al., 2009). However, in contrast to the *trol* mutants, these HS biosynthetic mutants showed an increase of eEJP amplitude. Furthermore, the NMJ of these mutants displayed far broader abnormalities than that of *trol* mutants, such as disruptions of mitochondrial localization in the muscles, and an increase of stimulus-dependent endocytosis in the motoneurons. HS chains of all HSPGs, including syndecan, Dlp, and Trol, were affected in the NMJ of these mutants, which may explain such broader defects. In this study, our data suggested that both the Trol core protein and HS chains contribute to the muscle growth and NMJ development. Thus, the interplay between the core proteins and their attached HS chains might determine the specificity of HSPG activities. Furthermore, HS chains are structurally diverse polysaccharides that display different affinities for various morphogens and growth factors (Maeda et al., 2011). Each synaptic HSPG may be decorated with HS chains with specific structures and thus regulates a distinct set of signaling molecules.

Irie et al. (2012) produced *Ext1* conditional knockout (KO) mice, in which HS biosynthesis was disrupted selectively in the glutamatergic neurons in the forebrain. In the pyramidal neurons of these KO mice, the evoked excitatory postsynaptic currents were remarkably depressed, and the frequency and amplitude of the miniature excitatory postsynaptic current were also reduced. Furthermore, the level of postsynaptically localized AMPA-type glutamate receptors was significantly reduced in this KO mouse. Such postsynaptic defects are similar to those of *trol* mutants observed in this study. The postsynaptic HSPGs expressed by the pyramidal neurons may regulate postsynaptic glutamate sensitivity by modulating Wnt signaling and/or ECM structures.

In the vertebrate NMJ, many Wnt family members are expressed by both motor neurons and muscle fibers, which play important roles in the motor growth cone guidance and acetylcholine receptor clustering at the NMJ (Strochlic et al., 2012; Zhang et al., 2012). However, *perlecan*-null mice showed only limited defects at the NMJ. Although acetylcholinesterase was absent at the NMJ of these KO mice, the early innervation pattern and acetylcholine receptor clustering were not significantly affected (Arikawa-Hirasawa et al., 2002). Because two HSPGs, agrin and perlecan, are attached to the postsynaptic membrane through dystroglycan (Singhal and Martin, 2011), agrin may provide compensatory support to Wnt signaling at the NMJ in *perlecan*-null mice. In fact, Henriquez et al. (2008) demonstrated that Wnt3 induces acetylcholine receptor aggregation at vertebrate neuromuscular synapses in collaboration with agrin. Recently, it has been proposed that Wnt and BMP/TGF-β signalings are involved in various neurodegenerative diseases, such as amyotrophic lateral sclerosis and Huntington's disease (Inestrosa and Arenas, 2010; Bayat et al., 2011). HSPGs, including perlecan, might be involved in the pathological mechanism of these diseases by modulating BMP/TGF-β and Wnt signalings. In this context, *trol* mutants may be useful as a model system to elucidate the involvement of HSPGs in the pathogenesis of neurodegenerative diseases.

In conclusion, our analyses demonstrate that Trol spatially regulates Wg activity in the NMJ synapses. There is growing evidence that neuronal activity induces the release of Wnt proteins at synapses in both vertebrate hippocampal neurons and *Drosophila* NMJs (Ataman et al., 2008; Gogolla et al., 2009). It is attractive to speculate that Trol/perlecan controls neuronal activity-dependent signaling of Wg/Wnt. Additional studies will be required to elucidate the roles of Trol in Wg-mediated synapse plasticity.

Materials and methods

Fly stocks

Flies were raised on standard media at 25°C. wg^{CX4}, htl^{AB42}, *elav-Gal4*, *OK6-Gal4*, *24B-Gal4*, *repo-Gal4*, and *UAS-sgg*^{act} (Bourouis, 2002) flies were obtained from the Bloomington *Drosophila* Stock Center, $trol^{ZCL1700}$ was obtained from the *Drosophila* Genetic Resource Center (Guha et al., 2009), *UAS-trol dsRNA* and *UAS-sfl dsRNA* were purchased from the Vienna *Drosophila* RNAi center, *UAS-GFP-wg* flies were obtained from S. Cohen (Institute of Molecular and Cell Biology, Singapore), $trol^{null}$ flies were obtained from H. Jäckle (Max Planck Institute for Biophysical Chemistry, Gottingen, Germany; Voigt et al., 2002), $trol^{7}$ flies were provided by S. Datta (Texas A&M University, College Station, TX; Park et al., 2003), *UAS-sec-dally* was obtained from H. Nakato (University of Minnesota, Minneapolis, MN; Takeo et al., 2005), gbb^{1} was obtained from K.A. Wharton (Brown University, Providence, RI), *UAS-dsh*^{DIX} was obtained from J. Axelrod (Stanford University School of Medicine, Stanford, CA; Axelrod et al., 1998), and *UAS-myc-NLS-DFz2-C* flies were provided by V. Budnik (University of Massachusetts Medical School, Worcester, MA; Mathew et al., 2005). All experiments were conducted in accordance with the Guideline for the Care and Use of Animals (Tokyo Metropolitan Institute of Medical Science, 2011).

Immunocytochemistry

Wandering third-instar larvae were used unless otherwise specified. Larval body wall muscles were dissected in Ca^{2+}-free HL3 saline (70 mM NaCl, 5 mM KCl, 20 mM $MgCl_2$, 10 mM $NaHCO_3$, 5 mM trehalose, 115 mM sucrose, and 5 mM Hepes, pH 7.2) and fixed in either Bouin's fixative or 4% paraformaldehyde/PBS for 20 min. Larvae were incubated overnight at 4°C in primary antibodies and then for 2 h at room temperature in secondary antibodies. All incubation and washing steps were performed in PBT (PBS + 0.3% Triton X-100). Extracellular labeling of Wg protein was performed according to Strigini and Cohen (2000). In brief, dissected body wall muscles of *OK6-Gal4/UAS-GFP-Wg* were incubated for 2 h at 4°C with anti-GFP antibody (1:10 dilution; MBL International) in HL3 saline. Body wall muscles were rinsed three times with ice-cold HL3 and fixed for 20 min in ice-cold PBS containing 4% paraformaldehyde. Subsequent processing was the same as in the conventional protocol except

no detergent was used. Degradation of HS was performed by incubation of body wall muscles with 100 mU/ml heparitinase I (Seikagaku) in HL3 saline for 1 h at 28°C. Extracellular labeling of HS was performed using the anti-HS antibody (10E4; Seikagaku) with the same protocol as the extracellular Wg labeling technique. The following primary antibodies were used: Cy5-conjugated goat anti-HRP (Jackson ImmunoResearch Laboratories, Inc.), mouse anti-DLG (4F3; Developmental Studies Hybridoma Bank), mouse anti-BRP (nc82; Developmental Studies Hybridoma Bank), anti-Futsch (22C10; Developmental Studies Hybridoma Bank), rabbit anti-GluRIIA (DM2; Saitoe et al., 1997), rabbit anti-GFP (MBL International), rabbit anti–α-Tubulin (Sigma-Aldrich), and rabbit anti–DFz2-C (Mathew et al., 2005). Alexa Fluor 488–, Alexa Fluor 546–, or Alexa Fluor 647–conjugated secondary antibodies were used at 1:250 (Invitrogen). Larvae were mounted in mounting medium (Vectashield; Vector Laboratories), and single or z stacks of NMJs were imaged at room temperature using a confocal microscope (TCS SP5; Leica; HCX Plan Apochromat 63×, 1.4 NA oil immersion objective lens) with LAS AF software (Leica). Image brightness and contrast were adjusted, and separate panels were assembled with Photoshop software CS Ver. 8.0.1 (Adobe). Fluorescent intensities for GluRIIA and Wg were measured using ImageJ software (National Institutes of Health).

Behavioral assay and electrophysiology

First- and third-instar larvae of wild type and *trol*^{null} were placed on an agar plate. The number of body wall contractions during 1 min was counted. Electrophysiology was performed on late third-instar larvae of wild-type and *trol*^{null} mutants. Filleted larvae were washed in HL3 saline containing 1.8 mM Ca^{2+} before recording. Recording electrodes were heat-pulled glass capillaries with resistances between 10 and 40 MΩ, filled with 3 M KCl. mEJPs and eEJPs were recorded in the bridge mode using an amplifier (AxoClamp-2B; Axon Instruments). The low pass filter was set at 1 kHz on the amplifier. Recordings were performed on muscle 6 in abdominal segments 2 and 3. Only those muscles with a resting membrane potential less than −60 mV throughout the recording were considered. Spontaneous events were recorded in the presence of 10 µM tetrodotoxin for 3 min, and these mEJP traces were analyzed by hand using the program of pClamp 9.2 software (Axon Instruments). Quantal content was estimated by dividing the mean eEJP by the mean mEJP.

Electron microscopy and immunoelectron microscopy

Body wall muscles of third-instar larvae of wild type and *trol*^{null} were prepared for transmission electron microscopy as described previously (Jia et al., 1993; Packard et al., 2002). In brief, body wall muscles were fixed in 1% glutaraldehyde, 4% paraformaldehyde, and 0.1 M sodium phosphate buffer, pH7.4, for 40 min at room temperature and then 4°C overnight. After washing in 0.1 M sodium phosphate buffer, pH 7.4, samples were postfixed for 1 h in 1% osmium tetroxide, stained with 2% uranyl acetate, dehydrated through a graded series of ethanol, and embedded in Quetol 812 (Nisshin EM). Ultrathin sections (60–80-nm thickness) were cut from the embedded samples with an ultramicrotome (EM UC7; Leica), collected on Formvar-coated copper grids, and contrasted with lead citrate. Synaptic boutons between muscles 6 and 7 were examined using a transmission electron microscope (JEM 1400; JEOL) with an accelerating voltage of 80 kV and imaged with a built-in digital charge-coupled device camera at 10,000× magnification. The size of the bouton and SSR was measured using ImageJ software. Immunoelectron microscopy of *trol*^{ZCL1700} third-instar larvae was performed using a preembedding technique. In brief, dissected larvae were fixed in 4% paraformaldehyde/0.1% glutaraldehyde/PBS and incubated with the anti-GFP antibody (1:300) followed by anti–rabbit IgG 1.4-nm nanogold (1:50; Nanoprobes). After intensification using HQ silver reagents (Nanoprobes), the samples were processed for electron microscopy as described in this paragraph.

Statistical analysis

For statistical analyses, we used Prism 4 (GraphPad Software). Numerical data are presented as means ± SEM. The nonparametric Mann–Whitney test was used to determine differences between two groups, and Kruskal–Wallis nonparametric analysis of variance and Dunn's post hoc test were used for multiple group comparisons.

Online supplemental material

Fig. S1 shows that the expression of *DFz2-C–NLS* did not rescue the defects of larval locomotion of *trol*^{null} and electrophysiological properties of their NMJs. Fig. S2 shows that NMJs of *sfl*^{null} mutants showed normal levels of GluRIIA expression. Fig. S3 shows that reduction of FGF signaling did not affect the *trol*^{null} mutant phenotype. Fig. S4 shows that ∼60% of HS was degraded after heparitinase treatment of the NMJ. Online supplemental material is available at http://www.jcb.org/cgi/content/full/jcb.201207036/DC1.

We thank Drs. J. Axelrod, V. Budnik, S. Cohen, S. Datta, H. Jäckle, H. Nakato, and K.A. Wharton and the Developmental Studies Hybridoma Bank, Bloomington *Drosophila* Stock Center, *Drosophila* Genetic Resource Center, and Vienna *Drosophila* RNAi Center for fly stocks and reagents. We are also grateful to the Center for Basic Technology Research at the Tokyo Metropolitan Institute of Medical Science for assistance with electron microscopy.

This work was partly supported by the Takeda Science Foundation, the Naito Foundation, and the Ministry of Education, Culture, Sports, Science and Technology of Japan/the Japan Society for the Promotion of Science KAKENHI grants numbers 24110521 and 22570149.

Submitted: 5 July 2012
Accepted: 14 December 2012

References

Arikawa-Hirasawa, E., S.G. Rossi, R.L. Rotundo, and Y. Yamada. 2002. Absence of acetylcholinesterase at the neuromuscular junctions of perlecan-null mice. *Nat. Neurosci.* 5:119–123. http://dx.doi.org/10.1038/nn801

Ataman, B., J. Ashley, D. Gorczyca, M. Gorczyca, D. Mathew, C. Wichmann, S.J. Sigrist, and V. Budnik. 2006. Nuclear trafficking of *Drosophila* Frizzled-2 during synapse development requires the PDZ protein dGRIP. *Proc. Natl. Acad. Sci. USA*. 103:7841–7846. http://dx.doi.org/10.1073/pnas.0600387103

Ataman, B., J. Ashley, M. Gorczyca, P. Ramachandran, W. Fouquet, S.J. Sigrist, and V. Budnik. 2008. Rapid activity-dependent modifications in synaptic structure and function require bidirectional Wnt signaling. *Neuron*. 57:705–718. http://dx.doi.org/10.1016/j.neuron.2008.01.026

Axelrod, J.D., J.R. Miller, J.M. Shulman, R.T. Moon, and N. Perrimon. 1998. Differential recruitment of Dishevelled provides signaling specificity in the planar cell polarity and Wingless signaling pathways. *Genes Dev.* 12:2610–2622. http://dx.doi.org/10.1101/gad.12.16.2610

Bayat, V., M. Jaiswal, and H.J. Bellen. 2011. The BMP signaling pathway at the *Drosophila* neuromuscular junction and its links to neurodegenerative diseases. *Curr. Opin. Neurobiol.* 21:182–188. http://dx.doi.org/10.1016/j.conb.2010.08.014

Bourouis, M. 2002. Targeted increase in shaggy activity levels blocks wingless signaling. *Genesis*. 34:99–102. http://dx.doi.org/10.1002/gene.10114

Budnik, V., and P.C. Salinas. 2011. Wnt signaling during synaptic development and plasticity. *Curr. Opin. Neurobiol.* 21:151–159. http://dx.doi.org/10.1016/j.conb.2010.12.002

Dean, C., and T. Dresbach. 2006. Neuroligins and neurexins: linking cell adhesion, synapse formation and cognitive function. *Trends Neurosci.* 29:21–29. http://dx.doi.org/10.1016/j.tins.2005.11.003

Deguchi, Y., H. Okutsu, T. Okura, S. Yamada, R. Kimura, T. Yuge, A. Furukawa, K. Morimoto, M. Tachikawa, S. Ohtsuki, et al. 2002. Internalization of basic fibroblast growth factor at the mouse blood-brain barrier involves perlecan, a heparan sulfate proteoglycan. *J. Neurochem.* 83:381–389. http://dx.doi.org/10.1046/j.1471-4159.2002.01129.x

Dietzl, G., D. Chen, F. Schnorrer, K.C. Su, Y. Barinova, M. Fellner, B. Gasser, K. Kinsey, S. Oppel, S. Scheiblauer, et al. 2007. A genome-wide transgenic RNAi library for conditional gene inactivation in *Drosophila*. *Nature*. 448:151–156. http://dx.doi.org/10.1038/nature05954

Friedrich, M.V., M. Schneider, R. Timpl, and S. Baumgartner. 2000. Perlecan domain V of *Drosophila melanogaster*. Sequence, recombinant analysis and tissue expression. *Eur. J. Biochem.* 267:3149–3159. http://dx.doi.org/10.1046/j.1432-1327.2000.01337.x

Fuki, I.V., R.V. Iozzo, and K.J. Williams. 2000. Perlecan heparan sulfate proteoglycan: a novel receptor that mediates a distinct pathway for ligand catabolism. *J. Biol. Chem.* 275:25742–25750. http://dx.doi.org/10.1074/jbc.M909173199

Gallet, A., L. Staccini-Lavenant, and P.P. Thérond. 2008. Cellular trafficking of the glypican Dally-like is required for full-strength Hedgehog signaling and wingless transcytosis. *Dev. Cell*. 14:712–725. http://dx.doi.org/10.1016/j.devcel.2008.03.001

Gogolla, N., I. Galimberti, Y. Deguchi, and P. Caroni. 2009. Wnt signaling mediates experience-related regulation of synapse numbers and mossy fiber connectivities in the adult hippocampus. *Neuron*. 62:510–525. http://dx.doi.org/10.1016/j.neuron.2009.04.022

Guha, A., L. Lin, and T.B. Kornberg. 2009. Regulation of *Drosophila* matrix metalloprotease Mmp2 is essential for wing imaginal disc:trachea association

and air sac tubulogenesis. *Dev. Biol.* 335:317–326. http://dx.doi.org/10.1016/j.ydbio.2009.09.005

Gumienny, T.L., L.T. MacNeil, H. Wang, M. de Bono, J.L. Wrana, and R.W. Padgett. 2007. Glypican LON-2 is a conserved negative regulator of BMP-like signaling in *Caenorhabditis elegans*. *Curr. Biol.* 17:159–164. http://dx.doi.org/10.1016/j.cub.2006.11.065

Henriquez, J.P., A. Webb, M. Bence, H. Bildsoe, M. Sahores, S.M. Hughes, and P.C. Salinas. 2008. Wnt signaling promotes AChR aggregation at the neuromuscular synapse in collaboration with agrin. *Proc. Natl. Acad. Sci. USA*. 105:18812–18817. http://dx.doi.org/10.1073/pnas.0806300105

Inestrosa, N.C., and E. Arenas. 2010. Emerging roles of Wnts in the adult nervous system. *Nat. Rev. Neurosci.* 11:77–86. http://dx.doi.org/10.1038/nrn2755

Irie, F., H. Badie-Mahdavi, and Y. Yamaguchi. 2012. Autism-like socio-communicative deficits and stereotypies in mice lacking heparan sulfate. *Proc. Natl. Acad. Sci. USA*. 109:5052–5056. http://dx.doi.org/10.1073/pnas.1117881109

Jia, X.X., M. Gorczyca, and V. Budnik. 1993. Ultrastructure of neuromuscular junctions in *Drosophila*: comparison of wild type and mutants with increased excitability. *J. Neurobiol.* 24:1025–1044. http://dx.doi.org/10.1002/neu.480240804

Johnson, K.G., A.P. Tenney, A. Ghose, A.M. Duckworth, M.E. Higashi, K. Parfitt, O. Marcu, T.R. Heslip, J.L. Marsh, T.L. Schwarz, et al. 2006. The HSPGs Syndecan and Dallylike bind the receptor phosphatase LAR and exert distinct effects on synaptic development. *Neuron*. 49:517–531. http://dx.doi.org/10.1016/j.neuron.2006.01.026

Kikuchi, A., H. Yamamoto, A. Sato, and S. Matsumoto. 2011. New insights into the mechanism of Wnt signaling pathway activation. *Int. Rev. Cell Mol. Biol*. 291:21–71. http://dx.doi.org/10.1016/B978-0-12-386035-4.00002-1

Kirkpatrick, C.A., B.D. Dimitroff, J.M. Rawson, and S.B. Selleck. 2004. Spatial regulation of Wingless morphogen distribution and signaling by Dally-like protein. *Dev. Cell*. 7:513–523. http://dx.doi.org/10.1016/j.devcel.2004.08.004

Koles, K., J. Nunnari, C. Korkut, R. Barria, C. Brewer, Y. Li, J. Leszyk, B. Zhang, and V. Budnik. 2012. Mechanism of evenness interrupted (Evi)-exosome release at synaptic boutons. *J. Biol. Chem.* 287:16820–16834. http://dx.doi.org/10.1074/jbc.M112.342667

Korkut, C., B. Ataman, P. Ramachandran, J. Ashley, R. Barria, N. Gherbesi, and V. Budnik. 2009. Trans-synaptic transmission of vesicular Wnt signals through Evi/Wntless. *Cell*. 139:393–404. http://dx.doi.org/10.1016/j.cell.2009.07.051

Kreuger, J., L. Perez, A.J. Giraldez, and S.M. Cohen. 2004. Opposing activities of Dally-like glypican at high and low levels of Wingless morphogen activity. *Dev. Cell*. 7:503–512. http://dx.doi.org/10.1016/j.devcel.2004.08.005

Lin, X. 2004. Functions of heparan sulfate proteoglycans in cell signaling during development. *Development*. 131:6009–6021. http://dx.doi.org/10.1242/dev.01522

Lindner, J.R., P.R. Hillman, A.L. Barrett, M.C. Jackson, T.L. Perry, Y. Park, and S. Datta. 2007. The *Drosophila* Perlecan gene trol regulates multiple signaling pathways in different developmental contexts. *BMC Dev. Biol.* 7:121. http://dx.doi.org/10.1186/1471-213X-7-121

Maeda, N., M. Ishii, K. Nishimura, and K. Kamimura. 2011. Functions of chondroitin sulfate and heparan sulfate in the developing brain. *Neurochem. Res.* 36:1228–1240. http://dx.doi.org/10.1007/s11064-010-0324-y

Mathew, D., B. Ataman, J. Chen, Y. Zhang, S. Cumberledge, and V. Budnik. 2005. Wingless signaling at synapses is through cleavage and nuclear import of receptor DFrizzled2. *Science*. 310:1344–1347. http://dx.doi.org/10.1126/science.1117051

McCabe, B.D., G. Marqués, A.P. Haghighi, R.D. Fetter, M.L. Crotty, T.E. Haerry, C.S. Goodman, and M.B. O'Connor. 2003. The BMP homolog Gbb provides a retrograde signal that regulates synaptic growth at the *Drosophila* neuromuscular junction. *Neuron*. 39:241–254. http://dx.doi.org/10.1016/S0896-6273(03)00426-4

Miech, C., H.U. Pauer, X. He, and T.L. Schwarz. 2008. Presynaptic local signaling by a canonical wingless pathway regulates development of the *Drosophila* neuromuscular junction. *J. Neurosci.* 28:10875–10884. http://dx.doi.org/10.1523/JNEUROSCI.0164-08.2008

Mosca, T.J., and T.L. Schwarz. 2010. The nuclear import of Frizzled2-C by Importins-β11 and α2 promotes postsynaptic development. *Nat. Neurosci.* 13:935–943. http://dx.doi.org/10.1038/nn.2593

O'Connor-Giles, K.M., L.L. Ho, and B. Ganetzky. 2008. Nervous wreck interacts with thickveins and the endocytic machinery to attenuate retrograde BMP signaling during synaptic growth. *Neuron*. 58:507–518. http://dx.doi.org/10.1016/j.neuron.2008.03.007

Packard, M., E.S. Koo, M. Gorczyca, J. Sharpe, S. Cumberledge, and V. Budnik. 2002. The *Drosophila* Wnt, wingless, provides an essential signal for pre- and postsynaptic differentiation. *Cell*. 111:319–330. http://dx.doi.org/10.1016/S0092-8674(02)01047-4

Packard, M., D. Mathew, and V. Budnik. 2003. Wnts and TGF β in synaptogenesis: old friends signalling at new places. *Nat. Rev. Neurosci.* 4:113–120. http://dx.doi.org/10.1038/nrn1036

Park, Y., C. Rangel, M.M. Reynolds, M.C. Caldwell, M. Johns, M. Nayak, C.J. Welsh, S. McDermott, and S. Datta. 2003. *Drosophila* perlecan modulates FGF and hedgehog signals to activate neural stem cell division. *Dev. Biol.* 253:247–257. http://dx.doi.org/10.1016/S0012-1606(02)00019-2

Pastor-Pareja, J.C., and T. Xu. 2011. Shaping cells and organs in *Drosophila* by opposing roles of fat body-secreted Collagen IV and perlecan. *Dev. Cell*. 21:245–256. http://dx.doi.org/10.1016/j.devcel.2011.06.026

Reichsman, F., L. Smith, and S. Cumberledge. 1996. Glycosaminoglycans can modulate extracellular localization of the wingless protein and promote signal transduction. *J. Cell Biol.* 135:819–827. http://dx.doi.org/10.1083/jcb.135.3.819

Ren, Y., C.A. Kirkpatrick, J.M. Rawson, M. Sun, and S.B. Selleck. 2009. Cell type-specific requirements for heparan sulfate biosynthesis at the *Drosophila* neuromuscular junction: effects on synapse function, membrane trafficking, and mitochondrial localization. *J. Neurosci.* 29:8539–8550. http://dx.doi.org/10.1523/JNEUROSCI.5587-08.2009

Rohrbough, J., E. Rushton, E. Woodruff III, T. Fergestad, K. Vigneswaran, and K. Broadie. 2007. Presynaptic establishment of the synaptic cleft extracellular matrix is required for post-synaptic differentiation. *Genes Dev.* 21:2607–2628. http://dx.doi.org/10.1101/gad.1574107

Saitoe, M., S. Tanaka, K. Takata, and Y. Kidokoro. 1997. Neural activity affects distribution of glutamate receptors during neuromuscular junction formation in *Drosophila* embryos. *Dev. Biol.* 184:48–60. http://dx.doi.org/10.1006/dbio.1996.8480

Saksela, O., D. Moscatelli, A. Sommer, and D.B. Rifkin. 1988. Endothelial cell-derived heparan sulfate binds basic fibroblast growth factor and protects it from proteolytic degradation. *J. Cell Biol.* 107:743–751. http://dx.doi.org/10.1083/jcb.107.2.743

Salinas, P.C., and Y. Zou. 2008. Wnt signaling in neural circuit assembly. *Annu. Rev. Neurosci.* 31:339–358. http://dx.doi.org/10.1146/annurev.neuro.31.060407.125649

Schuster, C.M., G.W. Davis, R.D. Fetter, and C.S. Goodman. 1996. Genetic dissection of structural and functional components of synaptic plasticity. I. Fasciclin II controls synaptic stabilization and growth. *Neuron*. 17:641–654. http://dx.doi.org/10.1016/S0896-6273(00)80197-X

Shishido, E., N. Ono, T. Kojima, and K. Saigo. 1997. Requirements of DFR1/Heartless, a mesoderm-specific *Drosophila* FGF-receptor, for the formation of heart, visceral and somatic muscles, and ensheathing of longitudinal axon tracts in CNS. *Development*. 124:2119–2128.

Singhal, N., and P.T. Martin. 2011. Role of extracellular matrix proteins and their receptors in the development of the vertebrate neuromuscular junction. *Dev. Neurobiol.* 71:982–1005. http://dx.doi.org/10.1002/dneu.20953

Strigini, M., and S.M. Cohen. 2000. Wingless gradient formation in the *Drosophila* wing. *Curr. Biol.* 10:293–300. http://dx.doi.org/10.1016/S0960-9822(00)00378-X

Strochlic, L., J. Falk, E. Goillot, S. Sigoillot, F. Bourgeois, P. Delers, J. Rouvière, A. Swain, V. Castellani, L. Schaeffer, and C. Legay. 2012. Wnt4 participates in the formation of vertebrate neuromuscular junction. *PLoS ONE*. 7:e29976. http://dx.doi.org/10.1371/journal.pone.0029976

Takeo, S., T. Akiyama, C. Firkus, T. Aigaki, and H. Nakato. 2005. Expression of a secreted form of Dally, a *Drosophila* glypican, induces overgrowth phenotype by affecting action range of Hedgehog. *Dev. Biol.* 284:204–218. http://dx.doi.org/10.1016/j.ydbio.2005.05.014

Toyoda, H., A. Kinoshita-Toyoda, B. Fox, and S.B. Selleck. 2000. Structural analysis of glycosaminoglycans in animals bearing mutations in sugarless, sulfateless, and tout-velu. *Drosophila* homologues of vertebrate genes encoding glycosaminoglycan biosynthetic enzymes. *J. Biol. Chem.* 275:21856–21861. http://dx.doi.org/10.1074/jbc.M003540200

Voigt, A., R. Pflanz, U. Schäfer, and H. Jäckle. 2002. Perlecan participates in proliferation activation of quiescent *Drosophila* neuroblasts. *Dev. Dyn.* 224:403–412. http://dx.doi.org/10.1002/dvdy.10120

Whitelock, J.M., J. Melrose, and R.V. Iozzo. 2008. Diverse cell signaling events modulated by perlecan. *Biochemistry*. 47:11174–11183. http://dx.doi.org/10.1021/bi8013938

Zhang, B., C. Liang, R. Bates, Y. Yin, W.C. Xiong, and L. Mei. 2012. Wnt proteins regulate acetylcholine receptor clustering in muscle cells. *Mol. Brain*. 5:7. http://dx.doi.org/10.1186/1756-6606-5-7